AD-A189 109 ON DYNAMIC LOADS IN PARALLEL SHAFT TRANSMISSIONS 2 1/1
PARAMETER STUDY(U) NATIONAL AERONAUTICS AND SPACE
ADMINISTRATION CLEVELAND OH LE.. H LIN ET AL. DEC 87
UNCLASSIFIED NASA-E-3756-2 NASA-TM-100101 F/G 20/11 NL

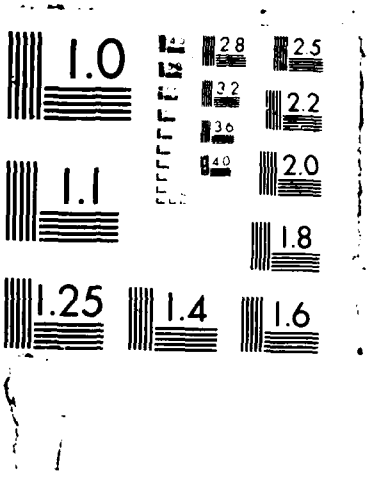
1.0
1.1
1.25
1.4
1.6
1.8
2.0
2.2
2.5
2.8
3.2
3.6
4.0

(2)

NASA
Technical Memorandum 100181

AVSCOM
Technical Report 87-C-3

On Dynamic Loads in Parallel Shaft Transmissions

II—Parameter Study

Hsiang-Hsi (Edward) Lin
Memphis State University
Memphis, Tennessee

Ronald L. Huston
University of Cincinnati
Cincinnati, Ohio

and

John J. Coy
Propulsion Directorate
U.S. Army Aviation Research and Technology Activity—AVSCOM
Lewis Research Center
Cleveland, Ohio

December 1987

NASA

US ARMY
AVIATION
SYSTEMS COMMAND
AVIATION R&T ACTIVITY

ON DYNAMIC LOADS IN PARALLEL SHAFT TRANSMISSIONS

II - PARAMETER STUDY

Hsiang-Hsi (Edward) Lin*
Department of Mechanical Engineering
Memphis, Tennessee 38152

Ronald L. Huston*
Department of Mechanical and Industrial Engineering
University of Cincinnati
Cincinnati, Ohio 45221-0072

and

John J. Coy*
Propulsion Directorate
U.S. Army Aviation Research and Technology Activity - AVSCOM
Lewis Research Center
Cleveland, Ohio 44135

SUMMARY

Solutions to the governing equations of a spur gear transmission model, developed in NASA TM-100180 (AVSCOM TM-87-C-2) are presented. Factors affecting the dynamic load are identified. It is found that the dynamic load increases with operating speed up to a system natural frequency. At operating speeds beyond the natural frequency the dynamic load decreases dramatically. Also, it is found that the transmitted load and shaft inertia have little effect upon the total dynamic load. Damping and friction decrease the dynamic load. Finally, tooth stiffness has a significant effect upon dynamic loading: the higher the stiffness, the lower the dynamic loading. Also, the higher the stiffness the higher the rotating speed required for peak dynamic response.

E-3757

INTRODUCTION

The development of a simple parallel shaft spur gear transmission model with its dynamic differential equations and solution procedures were presented in reference 1. Various parameters such as inertia, stiffness, friction and damping were included in the governing equations for further study (ref. 1).

The purpose of this report is to determine the effect of these parameters on gear dynamic load. The dynamic load of a gear transmission can be found by solving the governing equation. The solution is known as the dynamic motion of the gear transmission. This dynamic motion can then be substituted into other analytical formula and solved for gear dynamic loads.

---

*Member, ASME.

A model of the transmission is depicted in figure 1. The governing equations are:

$$J_M\ddot{\theta}_M + C_{s1}(\dot{\theta}_M - \dot{\theta}_1) + K_{s1}(\theta_M - \theta_1) = T_M \tag{1}$$

$$J_1\ddot{\theta}_1 + C_{s1}(\dot{\theta}_1 - \dot{\theta}_M) + K_{s1}(\theta_1 - \theta_M) + C_g(t)\,[R_{b1}\dot{\theta} - R_{b2}\dot{\theta}_2] + K_g(t)\,[R_{b1}(R_{b1}\theta_1 - R_{b2}\theta_2)] = T_{f1}(t) \tag{2}$$

$$J_2\ddot{\theta}_2 + C_{s2}(\dot{\theta}_2 - \dot{\theta}_1) + K_{s2}(\theta_2 - \theta_1) + C_g(t)\,[R_{b2}\dot{\theta}_2 - R_{b1}\dot{\theta}_1] + K_g(t)\,[R_{b2}(R_{b2}\theta_2 - R_{b1}\theta_1)] = T_{f2}(t) \tag{3}$$

$$J_L\ddot{\theta}_L + C_{s2}\,(\dot{\theta}_L - \dot{\theta}_2) + K_{s2}(\theta_L - \theta_2) = -T_L \tag{4}$$

where J_M, J_1, J_2, and J_L represent the mass moments of inertia of the motor, the gears, and the load; C_{s1}, C_{s2}, and $C_g(t)$ are damping coefficients of the shafts and the gears; K_{s1}, K_{s2}, and $K_g(t)$ are stiffness of the shafts and the gears; T_M, T_L, $T_{f1}(t)$, and $T_{f2}(t)$ are motor and load torques and frictional torques on the gears; R_{b1} and R_{b2} are base circle radii of the gears; t is time, and the overdots indicate time differentiation.

In this report we present the results of numerical solutions of equations (1) to (4) for a typical transmission system. A flow chart outlining the numerical procedure is presented. Natural frequencies are determined. The dynamic load is determined. Finally, the dynamic factor, defined as the ratio of the dynamic load to the static load, is determined.[1] The results are calculated as functions of the rotating speed and roll angle for a variety of damping and stiffness conditions.

NOMENCLATURE

C_g damping coefficient of gear tooth mesh, N-sec (lb-sec)

C_s damping coefficient of shaft, N-m-sec (in.-lb-sec)

J_L polar moment of inertia of load, kg-m^2 (in.-lb-sec^2)

J_M polar moment of inertia of motor, kg-m^2 (in.-lb-sec^2)

J_1 polar moment of inertia of gear 1, kg-m^2 (in.-lb-sec^2)

---

[1]The term "dynamic factor" or "dynamic load factor" has been used inconsistently in the literature. The American Gear Manufacturer's Association (AGMA) dynamic factor K_v is used as a strength reduction factor and is defined as the maximum static load divided by the maximum dynamic load. This paper will follow the ISO convention which uses the dynamic factor K_d as a load/stress increasing factor. Therefore, $K_d = 1/K_v$.

J_2 polar moment of inertia of gear 2, kg-m^2 (in.lb-sec^2)

K_d dynamic factor

K_g stiffness of gear tooth, N-m/rad (in.-lb/rad)

K_s stiffness of shaft, N-m/rad (in.-lb/rad)

K_v AGMA dynamic factor, Kv = $1/K_d$

R_b base radius, mm (in.)

R_p pitch radius, mm (in.)

T_L torque on load, N-m (in.-lb)

T_M torque on motor, N-m (in.-lb)

T_{f1} torque on gear 1, N-m (in.-lb)

T_{f2} torque on gear 2, N-m (in.-lb)

W applied load, N (lb)

θ angular displacement, rad

$\dot{\theta}$ angular velocity, rad/sec

$\ddot{\theta}$ angular acceleration, rad/sec^2

ω_n natural frequency, Hz

ξ damping ratio

PROCEDURE

Figure 2 presents a flow chart of the computational procedure used in the parameter study. The procedure is the same as that outlined at the end of reference 1.

In conducting the analysis it is useful to compare the locations of the peak dynamic loads with the locations of the system natural frequencies (or critical speeds). The natural frequencies themselves may be obtained by examining the undamped equations of motion. These equations may be written in the matrix form:

$$[J]\,[\ddot{\theta}] + [K]\,[\theta] = [0] \tag{5}$$

where the inertia matrix [J] is

$$[J] = \begin{bmatrix} J_M & 0 & 0 & 0 \\ 0 & J_1 & 0 & 0 \\ 0 & 0 & J_2 & 0 \\ 0 & 0 & 0 & J_L \end{bmatrix} \tag{6}$$

and the stiffness matrix [K] is

$$[K] = \begin{bmatrix} K_{s1} & -K_{s1} & 0 & 0 \\ -K_{s1} & K_{s1} + (K_g)_{avg} R^2_{b1} & -(K_g)_{avg} R_{b1} R_{b2} & 0 \\ 0 & -(K_g)_{avg} R_{b1} R_{b2} & K_{s1} + (K_g)_{avg} R^2_{b2} & -K_{s2} \\ 0 & 0 & -K_{s2} & K_{s2} \end{bmatrix} \quad (7)$$

where $(k_g)_{avg}$ represents the average value of the gear mesh stiffness. It is taken as the sum of the discrete tooth stiffness values of a mesh cycle divided by the number of mesh positions in the cycle.

In the parameter study the system had identical gears with the following properties:

Number of teeth	36
Module, mm	3.18 (8 diametral pitch)
Pitch diameter, m (in.)	0.1143 (4.5)
Pressure angle, deg	20
Applied load, N (lb)	2670 (600)
Face width, m (in.)	0.0254 (1.0)
Moment of inertia, kg m^2 (in.-lb sec^2)	3.3323×10^{-3} (0.02947)
Average tooth stiffness, N m/rad (lb-in./rad)	3.991×10^5 (3.5355×10^6)
Damping ratio	0.10

The shaft stiffness and inertias were:

Shaft stiffness, N m/rad (in.-lb/rad)	1138.17 (10081)
Load inertia and motor inertia, kg m^2 (in.-lb sec2)	9.989×10^{-3} (each) (0.08841)

RESULTS

Using the aforementioned data in the gear system model shown in figure 1, the natural frequencies of the four degrees of freedom model were found to be

$$\omega_{n1} = 0 \text{ (rigid body mode)} \qquad \omega_{n2} = 1.49 \text{ Hz}$$
$$\omega_{n3} = 2.99 \text{ Hz} \qquad \omega_{n4} = 144.8 \text{ Hz} \quad (8)$$

The first three natural frequencies are well below tooth meshing frequencies and are therefore not of interest in this analysis (although they can still be excited by shaft eccentricity which is not modeled here). The fourth natural frequency matches tooth meshing frequency at the critical speed of 8688 rpm which is within the operating range of the gears.

Figure 3 shows the variation of dynamic load response for a pair of teeth as a function of roll angle. At speeds much lower than the critical speed, the dynamic load response is basically a static load sharing in phase with the stiffness change, superimposed with an oscillatory load at a frequency corresponding to the natural frequency.

At higher speed, close to the critical speed, the dynamic load variation becomes so abrupt that it produces tooth separation. The peak dynamic load is much higher than the static load and is very likely to be a source of gear noise and early surface fatigue.

Figure 4 shows the dynamic factor K_d as a function of operating speed. Prominent peaks (resonances) may be seen at speeds of 7650 and 4200 rpm. The larger peak 7650 rpm occurs at 88 percent of the calculated critical speed. The experimental work by Kubo (ref. 6) reported a similar result that the critical speed was found at about 90 percent of the calculated critical speed. The second peak at 4200 rpm is a nonlinear effect of the time varying tooth stiffness known as the parametric resonance. This parametric resonance frequency occurs at about one-half of the critical speed (ref. 2). For speeds above the critical speed, the dynamic response decreases steadily in the same manner as with elementary vibrating systems.

Figure 5 shows a three-dimensional representation of the system dynamic response. The horizontal axis represents the operating speed, and the contact position along the tooth profile. The total number of contact positions is 121. The vertical axis is the dynamic factor.

Figure 6 presents a contour plot of the system dynamic response. The shaded areas represent regions where tooth separation occurs. They are located in the double contact regions. At near resonance speeds the vibration amplitude exceeds the deflection of the meshing teeth, thus inducing tooth separation.

As the speed increases, the dynamic response also shows a phase shift towards the higher numbered contact positions. This phenomenon can be seen by noting that at speeds from 600 to 4200 rpm (one-half subharmonic), the maximum dynamic load occurs at double- to single-contact transitions (position 51) and gradually changes to single- to double-contact transitions (position 75). At speeds between one-half subharmonic and resonance the maximum peak stays near the single- to double-contact transitions. After the speed passes resonance, the major dynamic peak moves again towards higher contact positions on tooth profile with increasing speed.

Figure 7 shows the dynamic factor as a function of the transmitted loads for three different speeds. There is only a small decrease in dynamic factor with increased applied load.

Figure 8 shows the effect of damping on the dynamic load. It is seen that damping has its greatest effect near resonance frequencies.

Changes in shaft stiffness have a minor effect on the system dynamic response. However changes of tooth stiffness have a major effect on the response. Figure 9 shows that the higher the tooth stiffness the lower the dynamic response (dynamic factor). This is consistent with observations that as the tooth stiffness increases the effect of gear mass on the system dynamics is reduced. Figure 9 also shows that system resonance frequencies are increased as the tooth stiffness increases. This is a potentially useful effect for the design of gear systems.

The effect of shaft mass is assumed small compared to that of the gears. Figure 10 shows that as the gear inertia is reduced, the dynamic response is also reduced.

For gears with different diametral pitches, the dynamic response is different due to the change in contact ratio. Gears with a finer pitch have a higher contact ratio. Since the contact ratio is a measure of the duration of the load being shared by more than one pair of teeth, it has a significant effect on the system dynamic response.

Figure 11 shows a comparison between gears having different diametral pitches. The finer pitch gears, having a higher contact ratio, have a smaller dynamic load than the coarser pitch gears.

DISCUSSION

In 1927, A.A. Ross (ref. 3) introduced the following empirical formula for the dynamic factor k_v:

$$k_v = \frac{78}{(78 + \sqrt{v})} \tag{9}$$

where v is the pitch line speed measured in ft/min. This expression received acceptance as a standard factor used by the American Gear Manufacturer's Association (AGMA). In 1959, a similar factor for use with higher precision gears was introduced by Wellauer (ref. 4)

$$k_v = \left[\frac{78}{78 + \sqrt{v}}\right]^{1/2} \tag{10}$$

Equations (9) and (10) are recognized as being conservative when applied with very high precision gears. They are thought to predict dynamic loads which are higher than the actual loads.

Buckingham (ref. 5) has also developed an expression for the dynamic load in terms of the pitch line speed and the applied load. His formula is

$$W_d = W + [f_a(2f_b - f_a)]^{1/2} \tag{11}$$

where W_d is the dynamic load, W is the applied load and the factors f_a and f_b are

$$f_a = f_b f_c/(f_b + f_c) \quad \text{and} \quad f_b = 0.0000555\ EF + W \tag{12}$$

where F is the face width, E is the elastic constant, and f_c is

$$f_c = 0.00120\ [(R_1 + R_2)/R_1R_2]mv^2 \tag{13}$$

where R_1 and R_2 are the pitch radii of the gears and m is their effective mass. (In these expressions the units are in pounds and inches except for the pitch line speed which is measured in ft/min.)

Kubo (ref. 6) measured static and dynamic gear stresses on several high-precision spur gear systems. Kubo expressed the dynamic factor as the ratio of maximum dynamic to the maximum static stress. Since stress is proportional to load, Kubo's definition of dynamic factor is identical to that used here. Figure 12 shows a comparison of $(1/K_v)$ from the AGMA high-precision formula (eq. (10)), (W_d/W) from Buckingham's formula, Kubo's results, and the results of the computer simulation for an identical spur gear pair with 4 mm module, 25 teeth, 20° pressure angle, 15 mm face width, 131.5 kN/m applied load, and 207 GPa Young's modulus.

There is a good agreement between Kubo's result and the computer simulation.

CONCLUSIONS

From the foregoing results several conclusions may be stated:

1. For accurately made gears, the dynamic load is significantly affected by the contact ratio: for increased diametral pitch, that is, for high contact ratio gears, the dynamic load is decreased.

2. The tooth stiffness has a significant effect upon the dynamic load: the higher the stiffness the lower the dynamic load. Also, the higher the stiffness the higher the critical speed for peak response.

3. The dynamic load generally increases with the operating speed until a resonance is reached. The dynamic load decreases rapidly beyond the resonance.

4. Damping and friction decrease the dynamic load with the most dramatic effects occurring near the resonance frequencies.

5. The applied load has a relatively minor effect upon the dynamic factor.

6. Tooth separation -- leading to impact -- occurs in the double tooth contact region since the deflections are smallest in that region.

7. The dynamic factor is largest for contact points near the tooth tip.

8. The dynamic factor decreases with decreases in the gear body inertia. Shaft moment of inertia has a minimal effect upon the dynamic factor.

REFERENCES

1. Lin, H.H., Huston, R.L., and Coy, J.J., On Dynamic Loads in Parallel Shaft Transmissions. I - Modeling and Analysis. NASA TM-100180, 1987.

2. Nafeh, A.H., and Mook, D.T., Nonlinear Oscillations, Wiley, 1979, Chapt. 5.

3. Ross, A.A.: Tooth Pressures for High-Speed Gears. Machinery (NY), vol. 34, no. 2, Oct. 1927, pp. 110-112.

4. Wellauer, E.J.: An Analysis of Factors Used for Strength Rating of Helical Gears. J. Eng. Ind., vol. 82. no. 3, Aug. 1960, pp. 205-212.

5. Buckingham, E.: Analytical Mechanics of Gears. Dover, 1963.

6. Kubo, A.: Estimation of Gear Performance, Proceedings of the International Symposium on Gearing and Power Transmissions, Japan Society of Mechanical Engineers, Tokyo, 1981, pp. 201-206.

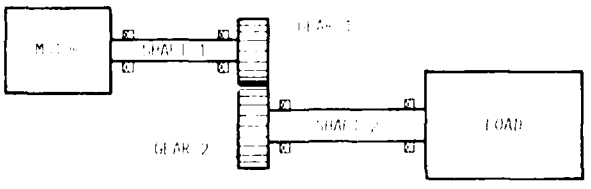

FIGURE 1. A SIMPLE SPUR GEAR SYSTEM.

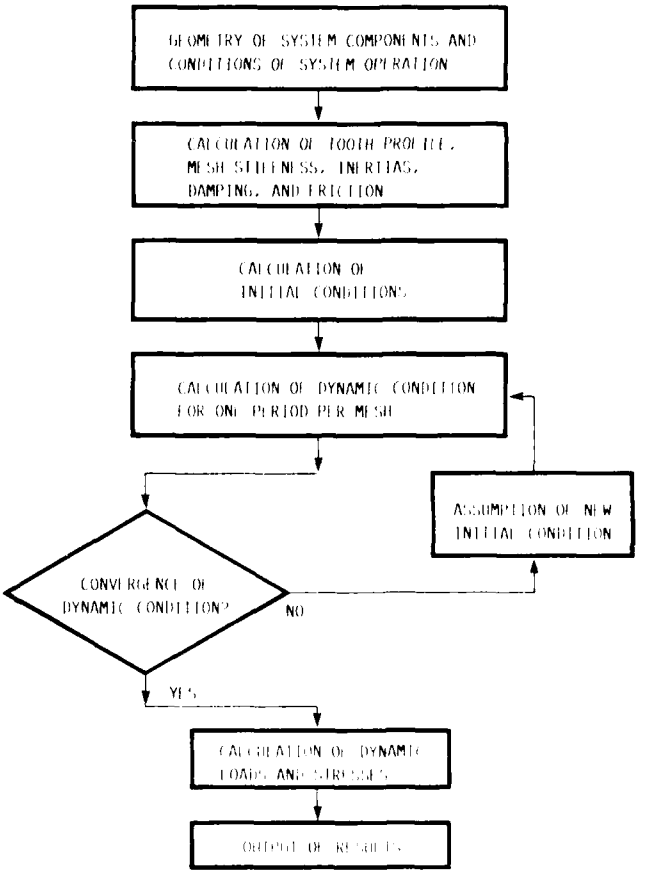

FIGURE 2. FLOW CHART OF COMPUTATIONAL PROCEDURE.

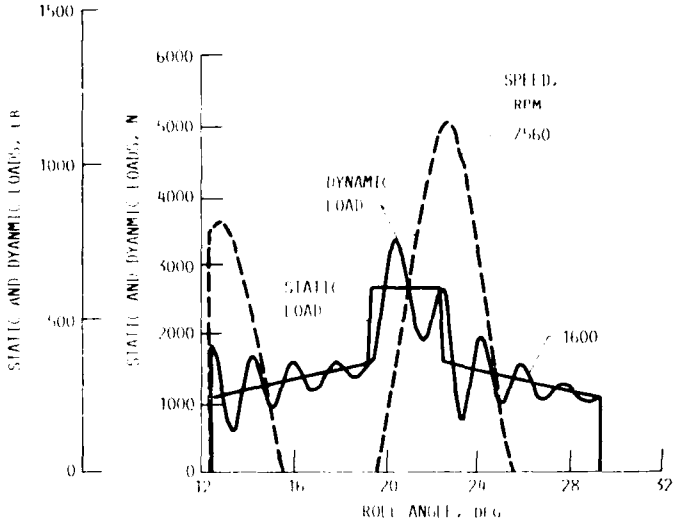

FIGURE 3. DYNAMIC LOADS AT DIFFERENT SPEEDS FOR IDENTICAL YEARS. MODULE 5.18 MM; PRESSURE ANGLE 20°; PITCH RADII 57.1 MM; APPLIED LOAD 2760 N (600 LB).

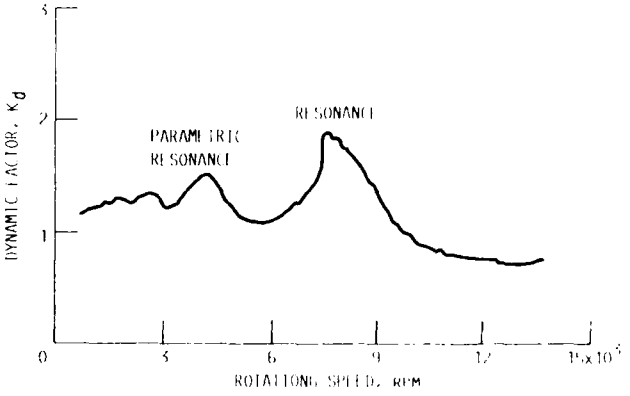

FIGURE 4. DYNAMIC FACTOR AS A FUNCTION OF ROTATING SPEED.

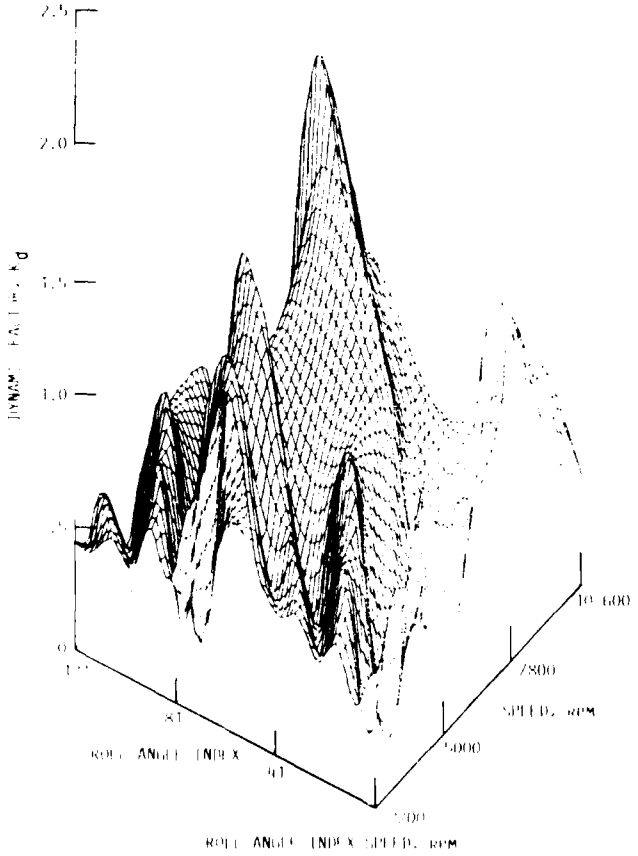

ROLL ANGLE INDEX SPEED, RPM

FIGURE 5. SYSTEM DYNAMIC RESPONSE.

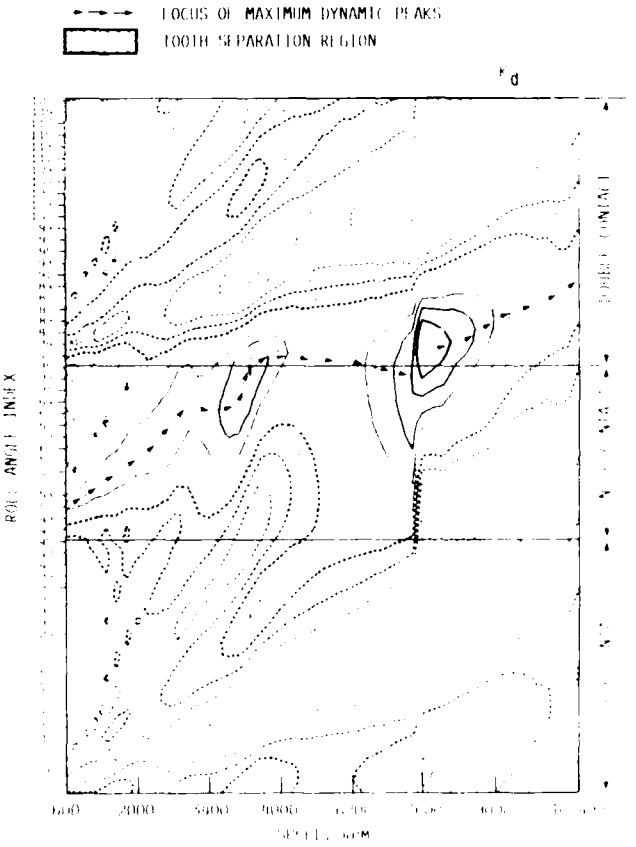

FIGURE 6. CONTOUR PLOT OF SYSTEM DYNAM[illegible]

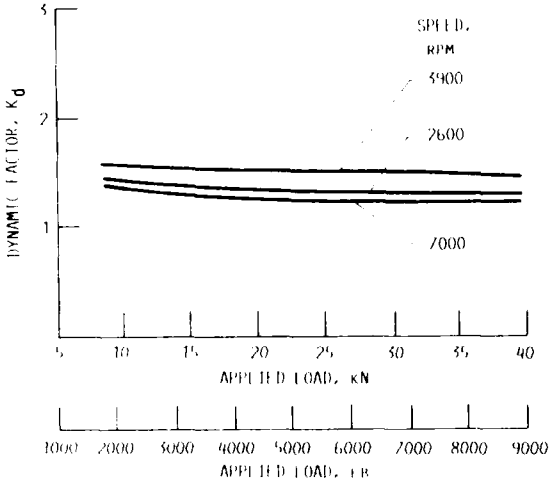

FIGURE 7. EFFECT OF APPLIED LOAD ON DYNAMIC RESPONSE.

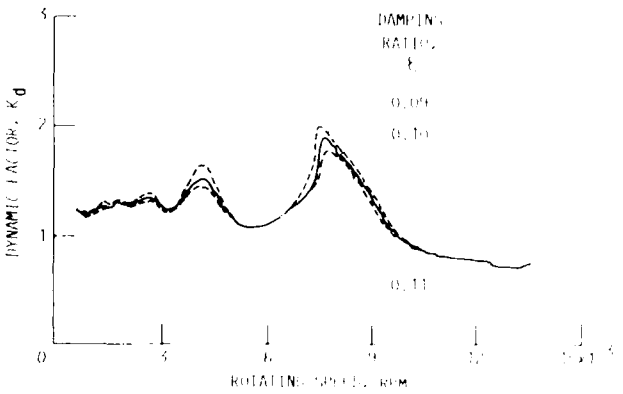

FIGURE 8. EFFECT OF DAMPING ON DYNAMIC [illegible]

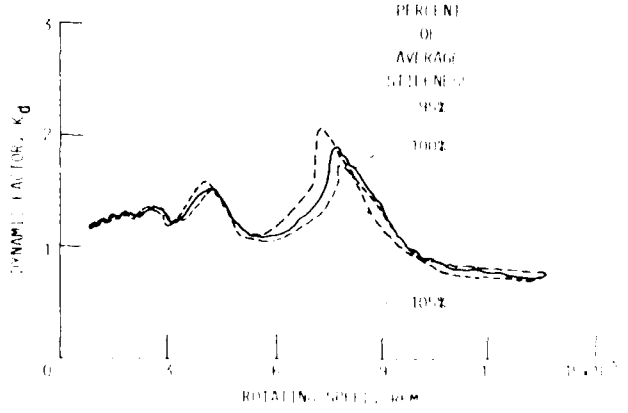

FIGURE 9. EFFECT OF AVERAGE TOOTH [illegible] ON DYNAMIC [illegible] RESPONSE. AVERAGE TOOTH [illegible] 100% VALUE [illegible] N-M/RAD.

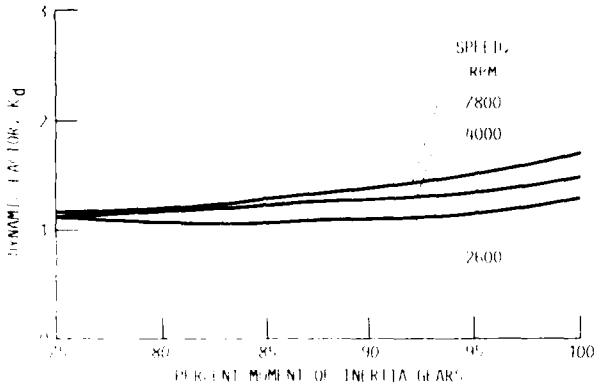

FIGURE 10. EFFECT OF GEAR INERTIA ON DYNAMIC ON DYNAMIC RESPONSE. GEAR INERTIA: 100% VALUE = 3.55×10^{-5} KG-M^2).

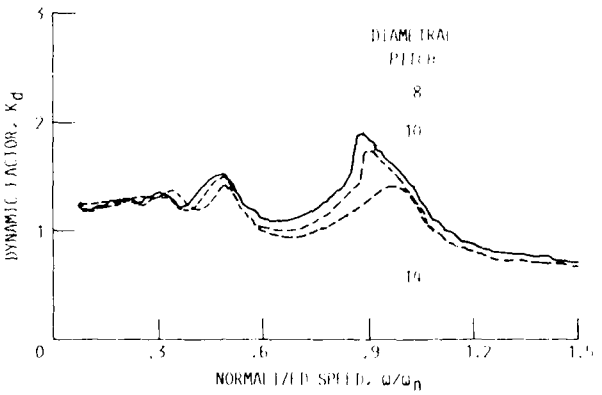

FIGURE 11. EFFECT OF DIAMETRAL PITCH ON DYNAMIC RESPONSE.

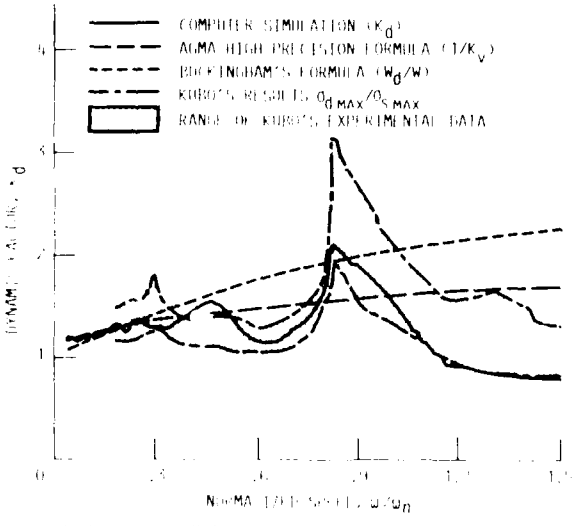

FIGURE 12. COMPARISON OF EXPERIMENTAL, EMPIRICAL, AND COMPUTER SIMULATION RESULTS.

NASA
National Aeronautics and Space Administration

Report Documentation Page

1. Report No.	2. Government Accession No.	3. Recipient's Catalog No.
NASA TM-100181 AVSCOM TM-87-C-3		

4. Title and Subtitle	5. Report Date
On Dynamic Loads in Parallel Shaft Transmissions II – Parameter Study	December 1987
	6. Performing Organization Code

7. Author(s)	8. Performing Organization Report No.
Hsiang-Hsi (Edward) Lin, Ronald L. Houston, and John J. Coy	E-3756
	10. Work Unit No. 505-63-51

9. Performing Organization Name and Address	11. Contract or Grant No.
NASA Lewis Research Center Cleveland, Ohio 44135-3191 and Propulsion Directorate U.S. Army Aviation Research and Technology Activity—AVSCOM Cleveland, Ohio 44135-3191	13. Type of Report and Period Covered Technical Memorandum
12. Sponsoring Agency Name and Address National Aeronautics and Space Administration Washington, D.C. 20546-0001 and U.S. Army Aviation Systems Command St. Louis, Mo. 63120-1798	14. Sponsoring Agency Code

15. Supplementary Notes

Hsiang-Hsi (Edward) Lin, Memphis State University, Dept. of Mechanical Engineering, Memphis, Tennessee 38152; Ronald L. Huston, University of Cincinnati, Dept. of Mechanical and Industrial Engineering, Cincinnati, Ohio 45221-0072; John J. Coy, Propulsion Directorate, U.S. Army Aviation Research and Technology Activity—AVSCOM.

16. Abstract

Solutions to the governing equations of a spur gear transmission model, developed in NASA TM-100180 (AVSCOM TM-87-C-2), are presented. Factors affecting the dynamic load are identified. It is found that the dynamic load increases with operating speed up to a system natural frequency. At operating speeds beyond the natural frequency the dynamic load decreases dramatically. Also, it is found that the applied load and shaft inertia have little effect upon the dynamic load. Damping and friction decrease the dynamic load. Finally, tooth stiffness has a significant effect upon dynamic loading: the higher the stiffness, the lower the dynamic loading. Also, the higher the stiffness the higher the rotating speed required for dynamic reponse.

17. Key Words (Suggested by Author(s))	18. Distribution Statement
Machine design Gears Vibration Transmissions	Unclassified – Unlimited Subject Category 37

19. Security Classif. (of this report)	20. Security Classif. (of this page)	21. No of pages	22. Price*
Unclassified	Unclassified	12	A02

*For sale by the National Technical Information Service, Springfield, Virginia 22161

END

DATE

FILMED

MARCH

1988

DTIC